ELSEVIER

Thin Solid Films 308–309 (1997) 436–442

thin Solid films

Thermal fatigue of hot work tool steel with hard coatings

C.M.D. Starling[a], J.R.T. Branco[b,*]

[a]*Department of Materials Engineering and Construction, School of Engineering, Federal University of Minas Gerais, Rua Espírito Santo, 35 Centro, 30160-030, Belo Horizonte, Minas Gerais, Brazil*
[b]*Technological Center of Minas Gerais Foundation-CETEC, Av. José Cândido da Silveira, 200 Cidade Nova, 31170-450, Belo Horizonte, Minas Gerais, Brazil*

Abstract

Relatively few studies have investigated the performance of coated tools at high temperatures. This is of interest for die casting and warm forging industries, where tool materials are expected to have high toughness, high tempering resistance and endure erosion, wear and thermal fatigue. This paper reports an investigation of the performance of AISI H13 tool steel, coated with TiN, CrN and duplex coatings, during thermal fatigue tests on a thermal cycling rig. During the testes, 20-mm long cylinders, with 10 mm diameter, were subjected to 500 high frequency induction heating and water cooling cycles, lasting 7 and 3 s, respectively. The thermal fatigue damage was evaluated by analyzing different crack dimensions and distribution by light microscopy. The results showed that the coatings increased thermal fatigue resistance. © 1997 Elsevier Science S.A.

Keywords: Thermal fatigue; Coatings; Hot work tool steel

1. Introduction

Various metal forming processes are carried out at temperatures higher than 0.5 times the homologous temperature, and are therefore considered hot working. Among them are die casting, continuous casting, hot forging and extrusion.

During hot working, tools and dies are subjected to thermal gradients. The core is kept colder than the surface. Heat flows from the work material to the die, heating the surface during the period when there is contact between them, while the entire die cools down during the removal of parts. Thermal gradients lead to dimensional variation which generate stress and deformation.

Fig. 1 illustrates, schematically, stress-strain cycles during hot work. It can be seen from this figure that two elastic deformations are involved: ϵ_{e2}, the elastic deformation at the maximum temperature, T_2 and ϵ_{e1}, the elastic deformation at the minimum temperature, T_1. In the first cycle the material is in a stress free condition. During the first heating cycle the evolution of stress follows O-A-B. In A the thermally induced stress intercepts the yield limit X temperature curve and follows it up to point B. During cooling from T_2 to T_1, the evolution follows B-C-D, which involves a compressive plastic deformation equal to ϵ_p. This compressive deformation is different from ϵ_{po}, the plastic deformation of the first heating cycle. Therefore, subsequent thermal cycles will follow the course B-C-D-E-B [1,2], eventually resulting in thermal fatigue [2]. This process is one of the main causes of die failure in hot working and is responsible for 70% of the failures in die casting [2].

Thermal fatigue nucleation and growth can be described by the Coffin-Manson and the Solomon equations, respectively [3]. These models indicate that the number of cycles to nucleate cracks, as well as their growth, vary exponentially with the plastic strain amplitude. Malm and Norstrom analyzed the relationship between plastic strain amplitude during thermal fatigue, (ϵ_p), and mechanical properties of materials [1]. They found:

$$\epsilon_p = \alpha(T_2 - T_1) - \frac{(1-\eta_2).\sigma_2}{E_2} - \frac{1-\eta_1.\sigma_1}{E_1} \quad (1)$$

where α is the thermal expansion coefficient, η, σ and E are the coefficients of Poisson, yield stress and Modulus of Elasticity, respectively. The indexes 1 and 2 correspond to T_1, and T_2, temperatures.

The Malm and Norstrom model indicates that high ther-

* Corresponding author. Tel.: +55 31 4892377 ext. 377; fax: +55 31 4892200; e-mail: jbranco@cetec.rmg.br

0040-6090/97/$17.00
PII S0040-6090(97)00600-7

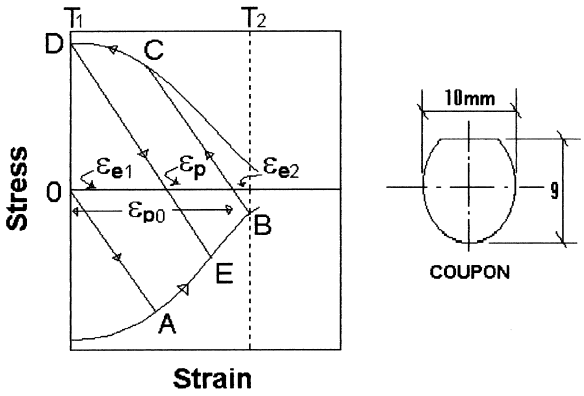

Fig. 1. Schematic stress-strain curve due to a thermal cycle between a low temperature, (T_1) and a high temperature (T_2). A cross section of a coupon sample is also shown.

mal fatigue resistant materials should have a low thermal expansion coefficient, a low Poisson coefficient and a high yield stress to Modulus of Elasticity ratio [4]. Oxidation resistance [5] and residual compressive stress [6] also contribute to raising the thermal fatigue resistance.

Some properties and characteristics of the hard coatings TiN and CrN (Table 1), suggest that they may contribute to raising the thermal fatigue resistance of a typical hot work steel. The higher chemical inertness of the coatings and the high residual compressive stresses, when produced by physical vapor deposition (PVD), should also help it. The combination of ion nitriding and hard coating may increase the thermal fatigue resistance even further because it provides better mechanical support to the hard coating than the tool steel. The nitriding layer also increase the depth of material with compression stress[7] and therefore should enhance thermal fatigue.

There are few papers on the thermal fatigue behavior of hard coatings. This paper looks into the damage caused by thermal cycling of AISI H13 hot work tool steel in four conditions: uncoated, coated with TiN, CrN and duplex coated (nitriding plus TiN).

2. Experimental procedures

A thermal fatigue testing unit was designed and built around the concept used by the Uddeholm Tooling Co. [14]. During each test, a coupon (Fig. 1), is cycled in a high frequency induction heating position and a water shower. The temperature at the coupon surface, sensored by a thermocouple, is monitored by a computer, which is programmed to control the heating and cooling cycle, either by temperature or time.

The thermal fatigue coupons were machined out of AISI H13 tool steel, quenched and tempered to 37 HRC. Four different conditions were tested (Table 2), one for each hard film, which were TiN, CrN, a duplex coating of TiN on top of a nitrided layer and an uncoated sample for control. Prior to coating, the flat surface of the samples were ground and polished to different roughness and subsequently cleaned in alcohol and acetone. The coatings were done by ion-plating, and the nitriding by a low pressure process [7], in a Balzers BAI 640 R unit. The initial surface roughness of samples was measured on the flat position of the coupons, along its symmetry axis (parallel) and perpendicular to it (transversal), (see Table 2). The substrates and coatings were examined by X-ray diffraction, light microscopy (LM) and scanning electron microscopy (SEM), before and after testing.

Each sample was subjected to 500 cycles between 50 and 720°C. The heating and cooling cycles lasted 6.7 and 3.5 s, respectively.

3. Results

The substrates used had a typical tempered martensite microstructure. X-ray diffraction of the coatings showed highly textured TiN and CrN with strong (111) orientation parallel to the substrate surface, and Ti and Cr, seen as layers by LM. The nitrided layer presented no iron carbides. Wide X-ray diffraction peaks were considered indicative of the presence of an amorphous phase, nanocrystals, non-homogeneous deformation or a combination of all three. After the thermal treatment a phase detected in the uncoated and CrN coated samples, had X-ray diffraction peaks corresponding to Fe_3O_4, but could not be identified conclusively. The observation of the tested H13 sample showed a black layer which would point to oxidation of the steel. The iron oxide expected to form around 720°C, the maximum temperature reached during the test, should be Fe_3O_4. Therefore, we concluded that Fe_3O_4 was present in the H13 and H13-CrN samples. The X-ray results also suggested the presence of the titanium oxide TiO_2 in the H13-TiN, but the results were not conclusive. No other evidences for the presence of TiO_2 in the coating were found. In the H13-CrN samples,

Table 1
Properties of ceramic films and other materials [8–13][a]

Property	H13	TiN	CrN	Fe-N[b]	Cr	Ti
Modulus of elasticity (MPa)	210 (145)	350 (600)		210	248	116
Thermal coefficient (10^{-6} K)	12	0.43		1	6.2	8.4
Hardness (HV)	500 (>100)	2000-2600 (1200)	2000-3000		1000	

[a]Properties at 750°C given between parenthesis. [b]Nitrided iron.

Table 2

Roughness of testing coupons (μm)

Material	Parallel	Transversal
H13	0.02	0.04
H13-TiN	0.17	0.06
H13-CrN	0.26	0.08
Duplex[a]	0.67	0.92

[a]TiN on top of nitrided layer.

Table 3

X-ray diffraction results of coupons samples, relative to the flat surface, before and after thermal cycling

Material	Before	After
H13	Fe	Fe, $Fe_2O_3^a$, $Fe_3O_4^a$
H13-TiN	Fe, Tia, TiN	Fe, Tia, TiN, TiO_2^a
H13-CrN	Fe, Cr, CrN	Fe, Cr, CrN, Cr_2N, $Fe_3O_4^a$
Duplex	Fe, Tia, TiN	Fe, Ti[a], TiN

CrN_2 was formed and the CrN X-ray peaks broadening decreased (Table 3).

To characterize the thermal fatigue resistance, the sample surfaces were compared under LM. The thermal fatigue tests successfully produced cracking with the same charac-

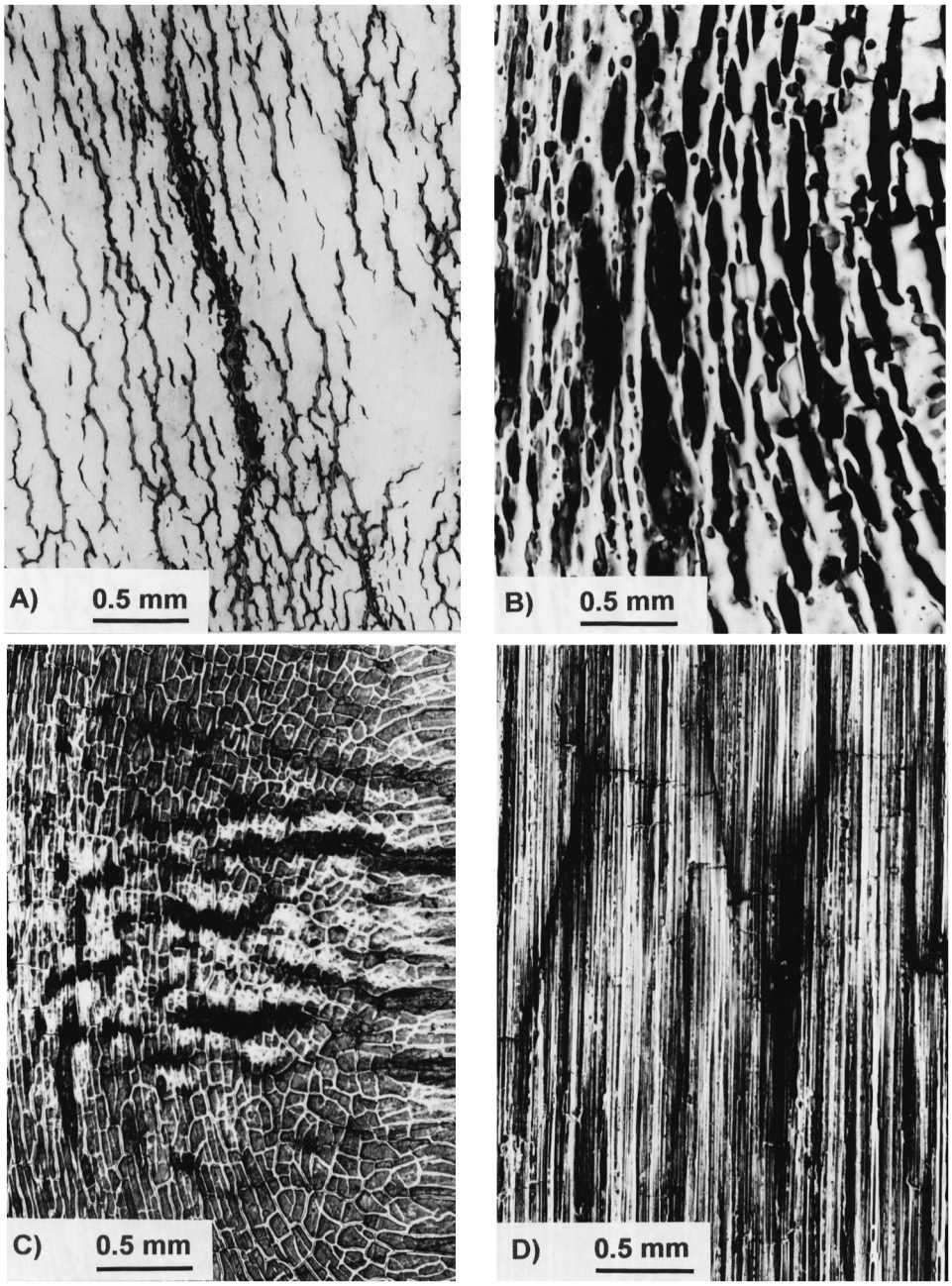

Fig. 2. Light micrograph of flat surfaces of thermal cycled coupon samples, carefully polished. No etching. (a) H13, (b) H13-TiN, (c) H13-CrN, (d) Duplex.

teristic pattern of the 'crazy cracking' found in hot working dies. The uncoated samples showed an oxide layer, which masked the cracking. A good contrast for crack observation was achieved by carefully polishing the oxide layer away (Fig. 2a). The coated samples showed no external sign of oxidation but coating spallation was noticed (Fig. 2). Except for the CrN coated samples, the coatings presented similar cracking patterns. Most cracks in the center part of the flat surface were parallel to the sample axis. Two levels of crack dimensions, each one with a distinct size distribution were present. At the SEM, the crack pattern showed up with better resolution (Fig. 3).

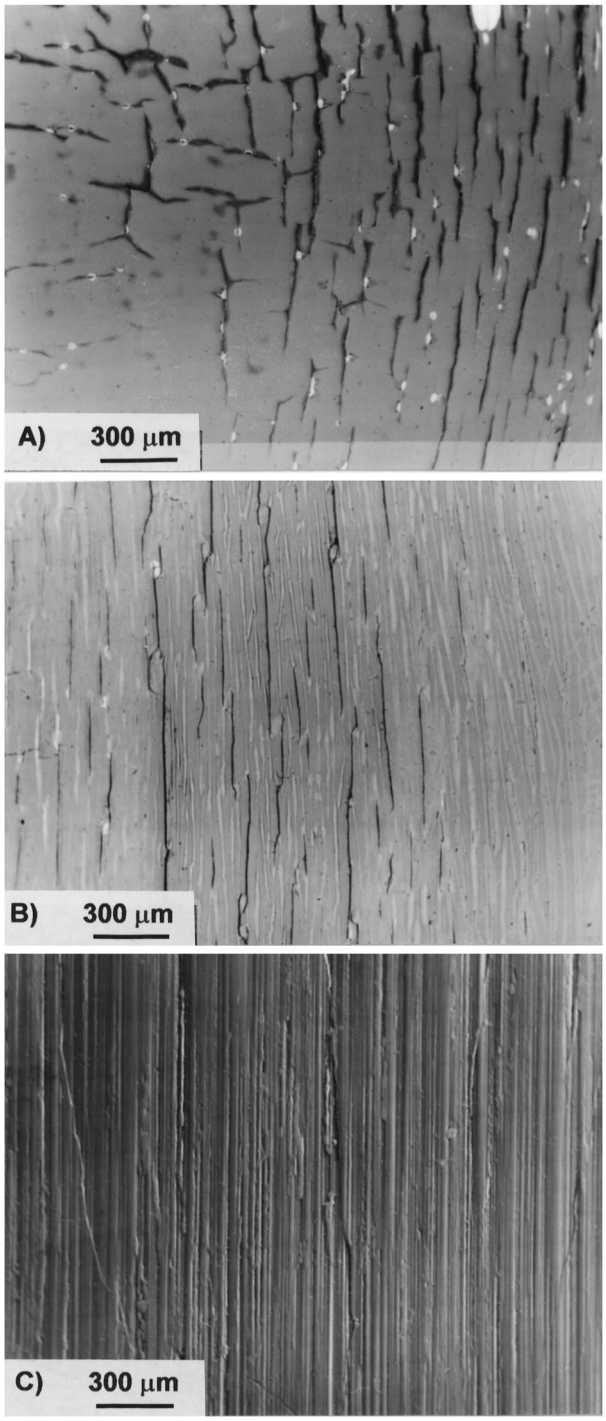

Fig. 3. Light micrograph of flat surfaces of thermal cycled coupon samples, carefully polished. No etching. (a) SEM: H13-TiN, (b) back scattered images: H13-CrN, COMPO contrast and (c) secondary electron image: Duplex.

The different oxidation resistance of the substrate and the coatings can be clearly seen in the cross sections (Fig. 4). First of all, we found no oxide at the surface of the coated samples. Substrate oxidation was visible only inside the substrate cracks. The higher the oxide volume the bigger the coating crack opening was. The oxides branch underneath the coating and when this happens, it is likely that a step is created at the surface. These results suggest that more cracking leads to more oxidation.

The thermal fatigue resistance was evaluated based on some crack size and density parameters, defined as:

- P_{max}, the maximum crack depth,
- $\sum P$, the accumulated crack depth,
- P_{med}, the average crack depth
- ρ, the number of cracks per unit of length.

The measurement of these parameters was done on cross sections of the tested samples, along the whole length of the surface edge, in the two halves. The coupons were cut perpendicular to their axis, in the center of the heated zone. The results are presented in Fig. 5.

4. Discussion

In a forming plant the dies are checked for cracks reaching a certain size and for crack density. There are different ways to assess this damage and likewise, the thermal fatigue performance of materials. Malm et al. proposed a method that requires a comparison between the crack network of the sample with two sets of reference charts, each rating from 1 to 10 [14]. An evaluation of the cracking pattern is done with a light microscope. In one chart there is a rating for the leading cracks, which are the deepest but with a low density. In the other chart the overall crack network is rated. This method could have been used (Fig. 2). However, it would be misleading because the sample cross sections showed that underneath the coating the substrate crack surface is highly oxidized. Therefore, the crack opening seen on the coated sample surface is much smaller than what is seen at the coating-substrate interface (Fig. 4).

Another possibility to assess thermal fatigue damage is to measure crack dimension parameters, like, for example, ρ, P_{med}, $\sum P$ and P_{max}, defined above. Similar to the procedure in a industrial plant, these parameters evaluate the largest crack as well as the crack network. The parameter that best indicates performance may vary with application.

Thermal fatigue occurs at the high stress end of the *S-N* curves, which corresponds to a low cycle fatigue [2]. During heating the sample surface expands and, due to the interac-

tion with the cold sample core, it is subjected to plastic compression. During cooling, the elongated surface will contract, which generates tensile stress on it (Fig. 1). The total deformation is given by:

$$\Delta\epsilon = \epsilon_e + \epsilon_p \quad (2)$$

However, under a low cycle regime, plastic strain is quantitatively more relevant than elastic strain, and the elastic strain can be neglected for modeling purpose. The strain amplitude (x) number of cycles curve shows the Manson-Coffin relationship [2]:

$$\Delta\epsilon_p = \acute{\epsilon}_f . N_f^{-3} \quad (3)$$

where N_f is the life, measured in number of cycles to failure, $\acute{\epsilon}_f$ is the fracture strain and β is a constant, called the fatigue ductility exponent.

The crack density, ρ, should increase with N_f [14], i.e.,

$$\rho = f(\Delta\epsilon_p / \acute{\epsilon}_f) \quad (4)$$

where $\Delta\epsilon_p$ increases with ΔT, the temperature variation in

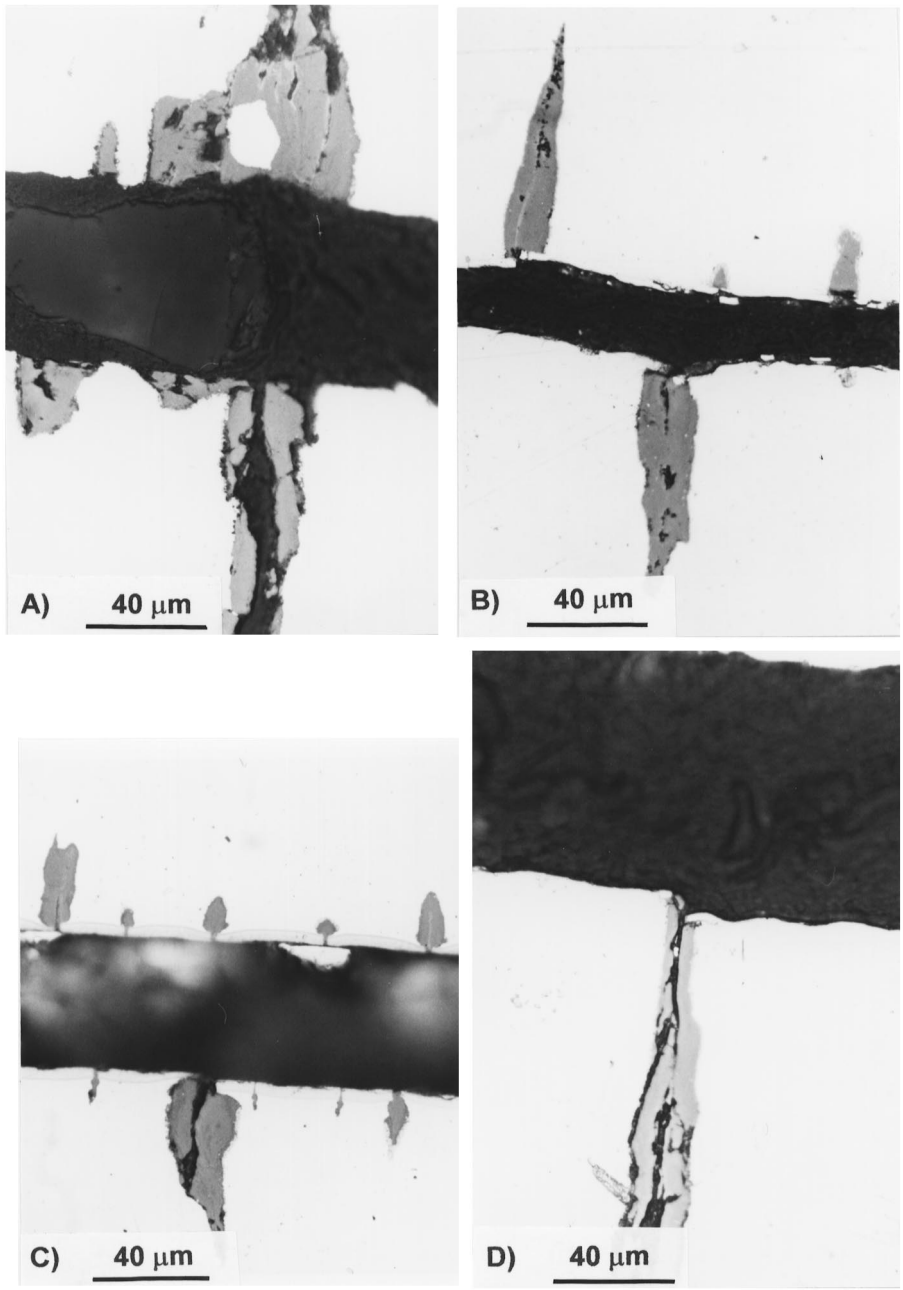

Fig. 4. Light micrographs of transversal sections of thermal cycled coupons. No etching. (a) H13, (b) H13-TiN, (c) H13-CrN, (d) Duplex.

the sample surface, and decreases with its hot yield strength. But the hot yield strength is proportional to the hot hardness, H_{ht}. Therefore:

$$\rho = f(\Delta T / H_{nt}\epsilon_f') \quad (5)$$

After initiation the fatigue crack grows, with a rate described by the Solomon equation:

$$da/dN = A(\Delta K)^n \quad (6)$$

when ΔK, the opening mode stress intensity factor, is above a threshold value. da/dN is the crack size increment per cycle and A is a proportionality constant. ΔK increases with stress amplitude which increases with ΔT.

Table 1 indicates the properties of the materials found in the literature. The hard coatings used are characterized by hot hardnesses significantly greater than that of the tool steel used, with higher tempering resistance than tool steels [8]. For example, TiN hot hardness is over 5 times higher than that of H13. On the other hand, ϵ_f' of hard coatings, even though unknown, is expected to be much lower than for the tool steel. However, the fact that the hard coatings used come with compression stresses, compensates the latter drawback. Taking all these facts into consideration one would expect the coated samples to have a lower crack density. This was true for the duplex sample but the H13 and the TiN sample had the same ρ, while the CrN sample had a higher density.

The different roughness values among the samples may be partially responsible for the different crack density observation. Higher roughness in the transversal direction increases the likelihood of surface cracks. Another relevant factor was the annealing and decomposition of CrN, as detected by x-ray diffraction, which decrease the coating hardness.

During heating, the coatings, which have lower thermal expansion coefficients than tool steels, will expand 10-20 times less than the substrate. To maintain coating-substrate continuity, the coated substrate will deform less than the uncoated one, which will result in a lower stress intensity factor and, consequently, a lower crack growth rate. Furthermore, the residual compressive stress in the coatings and nitrided layer reduce the stress intensity factor at the nucleated crack tip, reducing the crack growth rate in the substrate.

This effect seems to have been observed in the TiN sample, which showed lower P_{max}. CrN sample showed higher P_{max} than TiN, which may be related to the fact that it suffered significant annealing and phase transformation during thermal cycling. Furthermore, CrN coatings have lower residual stress. The uncoated and the Duplex coated samples showed the same P_{max} values, higher than the TiN and CrN samples. The poor Duplex performance may have been a consequence of its much higher surface roughness. In fact, a surface roughness effect on tool steel thermal fatigue resistance has been observed [15].

It is relevant that the thermal fatigue rating may have a big scatter [14], which can be >200 μm [16]. A correlation between the thermal fatigue rating and P_{max} has been suggested, which also indicates a big scatter in the results. For example, for a given ranking, P_{max} can vary from 200 to 1000 μm [14]. Therefore, even though the cracking parameters differ among the tested samples, the observed difference can not be considered big.

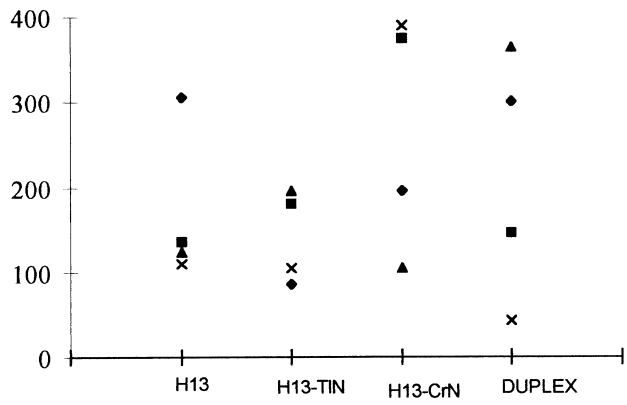

Fig. 5. Thermal fatigue rating results. (♦) *P*max (μm), (■) *P*/10 (μm), (●) 4*P*med (μm) and x 16 ρ (cracks/mm).

5. Conclusions

The hard coatings used can inhibit thermal fatigue. The mechanism was not disclosed yet but it is likely to involve both delaying crack nucleation and crack growth due to the coating high hot hardness and high residual compressive stress. This effect, combined with the high hardness of the coatings which reduces wear, may contribute to die life increase in hot work. A nitrided layer between TiN and the tool steel may enhance low cycle fatigue resistance even further.

Acknowledgements

The authors would like to thank the many people that contributed to this work, especially Forjas Acesita for supplying the materials, Balzers AG for the coatings, FAPEMIG for the financial support through the project TEC 446/90 and colleagues from the metallurgy department for their cooperation and patience.

References

[1] S. Malm and L-A. Norstrom, *Met. Sci*., (1979) 544.
[2] S.S. Manson, *Thermal Stress an Low-Cycle Fatigue*, McGraw Hill, New York, 1966.
[3] L. Liimatainen and A. Ranta-Eskila, *Die Cast. Eng*., 1991.
[4] G.E. Dieter, *Mechanical Metallurgy*, McGraw Hill, London, 1976.
[5] L. Kosec, F. Kosel and F. Vodopivec, *Proc.4th E.C.F. Conf*., Leoben, 1992, p.653.

[6] L. Eliasson and O. Sandberg,in H. Berns, H. Nordberg and H.-J. Fleishcer (eds.), *Proc. 2nd Int. Conf. Tooling*, Bochum, 1989, p. 3-14.
[7] N. Dingremont, E. Bergmann, P. Collignon and H. Michel, *Int. Conf. Metallurg. Coat. Thin Films*, April 1994.
[8] D.T. Quinto, G.J. Wolfe and P.C. Jindal, *Thin Solid Films, 153* (1987) 19.
[9] E. Torok, A. J. Perry, *Thin Solid Films, 153* (1987) 37.
[10] W.C. Oliver, C.J. McHargue and S.J. Zinkle, *Thin Solid Films, 153* (1987) 185.
[11] A.J. Perry, *Thin Solid Films, 193-194* (1990) 463.
[12] Metals Handbook, 9th ed., *Properties and Selections: Irons and Steels, Vol. 1*, 1978. ASM, Materials Park, OH, USA.
[13] Metals Handbook, 9th ed., *Properties and Selections: Nonferrous Alloys and Pure Metals, Vol. 2*, 1979. ASM, Materials Park, OH, USA.
[14] S. Malm, M. Svensson, and J. Tidlund, *Proc. 2nd Int. Colloq. Tool Steels Hot Working*, Saint-Etienne, 1977.
[15] I. Artinger and L. Becker, *Proc. 8th Congr. Mater. Test., Vol. II*, Budapest, 1982, p. 616-621.
[16] B.M. Gonzalez, J.E. da Silva and J.R.T. Branco, *Niobium Tool Steel - Thermal Fatigue Resistance*. Final Report. Technological Center of Minas Gerais Foundation, Belo Horizonte, 1985.